Int. J. Nano Dimens., 12 (4): 328-334, Autumn 2021

ORIGINAL ARTICLE

# Nano-filler Co-nanoparticles embedded in a Silica aerogel matrix

*Sapna Bakul Jadhav [1,2], Arwa Makki [3], Dina Hajjar [3], Pradip Bhikaji Sarawade [1,*]*

[1] *Department of Physics, University of Mumbai, Kalina, Mumbai-400098, India*
[2] *SDSM College, Palghar-401404, University of Mumbai, India*
[3] *University of Jeddah, Collage of Science, Department of Biochemistry-80327, Jeddah, KSA*

Received 04 March 2021; revised 06 May 2021; accepted 29 May 2021; available online 05 June 2021

**Abstract**

In present research, we synthesized cobalt-based silica nanocomposites (Co-$SiO_2$) from cobalt nitrate [$Co(NO_3)_2$] and tetraethoxysilane (TEOS) precursors by using a simple sol-gel method followed by supercritical drying techniques. The physicochemical and textual properties of the as synthesized nano composites were thoroughly investigated. The results indicated that the Co-$SiO_2$ aerogels demonstrated homogeneous dispersion cobalt nanoparticles within silica matrix with mesoporous morphology, large specific surface area (802 $m^2/g$) and larger pore size (9 nm) with less volume shrinkage. The physico-chemical properties of the cobalt based silica nanomaterial were characterized by XRD, SEM, $N_2$ adsorption-desorption and FTIR techniques. Cobalt-based silica nanocomposites can be produced using TEOS-based precursor and supercritical drying techniques. The prepared (Co-$SiO_2$) nanocatalyst due to its magnetic nature with higher surface area (802 $m^2/g$) can be utilized in many emerging fields such as catalysis, water desalination, water splitting, gas-sensing application and organic pollutant degradation.

**Keywords:** *Aerogel; Cobalt-Silica Nanocomposites; Nanocatalysts; Sol-gel Process; Supercritical Drying.*

**How to cite this article**

*S. Bakul Jadhav, A. Makki , D. Hajjar, P. Bhikaji Sarawade. Nano-filler Co-nanoparticles embedded in a Silica aerogel matrix. Int. J. Nano Dimens., 2021; 12(4): 328-334.*

## INTRODUCTION

The recent developments in nanocomposites materials and their promising properties make them potential candidates for various fields, such as wastewater treatment, medical industry, and so on [1-5]. Due to their most stable, stronger catalytic activity, and abundance in nature, nanoscale cobalt-based nanocomposites materials are the most promising catalyst for water splitting [6-8], organic pollutant decay [9], and toxic gas treatment [10].

Mesoporous $SiO_2$ aerogel accompanied with transition metal or metal-oxide nanoparticle diffused into the air-filled porous silica network is one of the demanding materials [11]. Systems based on metal/metal oxide dispersed in amorphous silica matrix have been recently proposed as catalysts or gas sensors for different reactions such as oxidation of benzene, Fisher-Tropsch synthesis, and air purification [12, 13]. Furthermore, the effect of the microstructure of $Co_3O_4$ based in porous silica material on water oxidation activity has been reported, and it was discovered that porous silica 20 nm thick boosts water oxidation activity [14].

Furthermore, the catalytic activity of $Co_3O_4$ nanoparticles is largely determined by their morphology, dispersion of cobalt oxide particles, and physicochemical properties. The sol-gel method is a significant way to obtain silica-supported $Co_3O_4$ catalysts, which contributes to considerable physicochemical properties of the $Co_3O_4$ nanomaterials. The sol-gel method and traditional time consuming ambient pressure drying (APD) methods uses a lot of resources [15,

* Corresponding Author Email: *pradip.sarawade@physics.mu.ac.in*

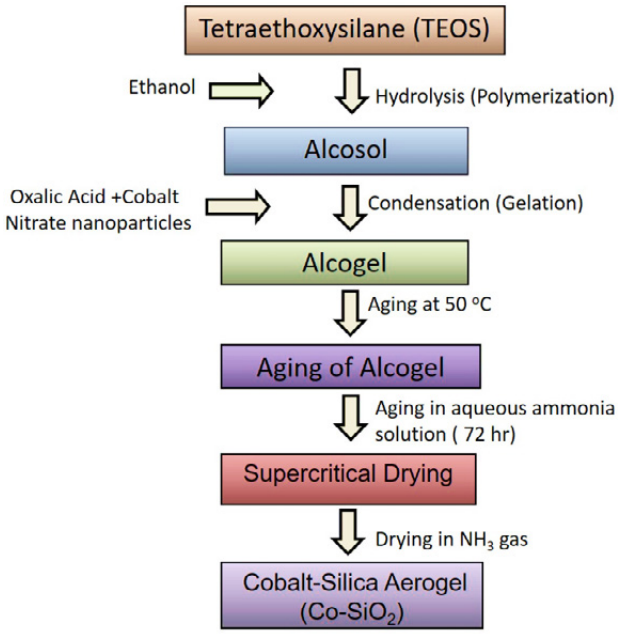


Fig. 1. Flowchart for the synthesis of Co-$SiO_2$ aerogel.

16]. Due to the time-consuming drying process and waste of large quantities of solvent exchange in APD [17-18] techniques, the aerogels marketability has been severely limited. Therefore supercritical drying (SCD) is a well-known alternative method for time consuming ambient pressure drying (APD) method.

We previously used [Ni $(NO_3)_2$] as a nanofiller implant in a silica matrix to investigate the surface properties of Ni-$SiO_2$ composites [19]. In the present studies, by using simple sol-gel process we could control effectively the larger pore sizes of TEOS-based Co-based silica aerogels with extremely high surface area (802 $m^2/g$) and large pore volume (2.9 $cm^3/g$) could be synthesized by supercritical drying techniques.

## EXPERIMENT

*Materials and methods*

Tetraethylorthosilicate (TEOS) was used as a precursor, analytical reagent, ammonium hydroxide ($NH_4OH$, 0.1M), Ethanol ($C_2H_5OH$), Oxalic acid (0.001 M) as a catalyst, and Cobalt nitrate hexahydrate [$Co(NO_3)_2.6H_2O$] salt. Without further purification, all reagents and chemicals were used. Double distilled water was used to dilute the concentration of oxalic acid and ammonium hydroxide catalysts.

*Synthesis of colloidal emulsions of cobalt oxide particles into nanoporous $SiO_2$ matrix*

Co–$SiO_2$ aerogels were prepared by two step acid–base catalysed sol–gel method followed by supercritical drying techniques. A flowchart for the synthesis of Co-$SiO_2$ aerogel nanocomposite is shown in Fig. 1. The aerogels were prepared in 200 ml beaker in two steps process as follows: in first step acid catalyzed sol was prepared by dissolving cobalt nitrate hexahydrate salt (0.8 g) into the aqueous oxalic acid (5.5 mL) solutions (Fig. 2a). In subsequent steps TEOS precursor and EtOH added drop by drop with continuous stirring to the acid catalyzed sol. In the second step, the base catalyst ($NH_4OH$) was added drop by drop while stirring at 6 hours of time interval to the acid catalyzed sol.

The molar ratio of TEOS : EtOH : $H_2O$ (acid) : $H_2O$ (basic) was kept constant at 1 : 3.5 : 3.9 : 2.1 along with the oxalic acid and $NH_4OH$ concentrations constant at 0.01 and 0.5 M, respectively. The alcogels were then transferred to 100 ml beakers and they were made air-tight and were kept for gelation at room temperature. After the sols were set (Fig. 2b), a small amount of ethanol was added over the gels in order to prevent the evaporation of pore solvent and thereby the shrinkage of the gel. Further the alcogels was aged in alcohol (ethanol) at room temperature for 6 hours. Finally, the

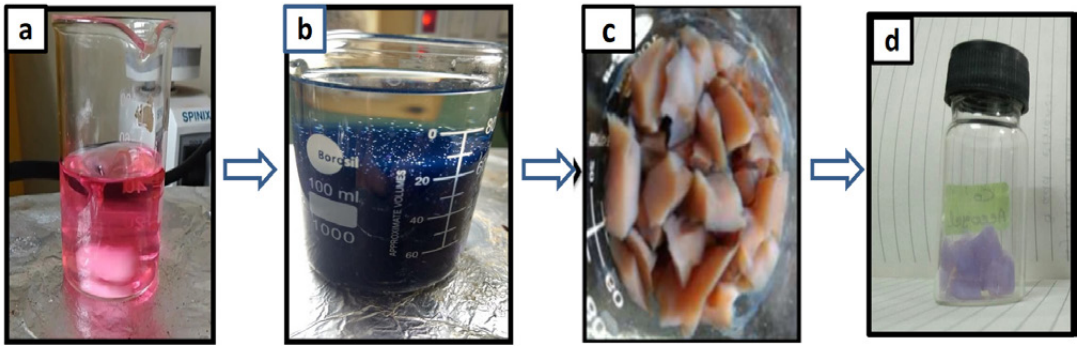


Fig. 2. Photographs of a) Silica sol with cobalt nitrate nanoparticles b) Addition of ammonia c) Supercritical dried and d) After calcinations-silica aerogels nano-composites (calcinations at 500 ºC for 6 hr).

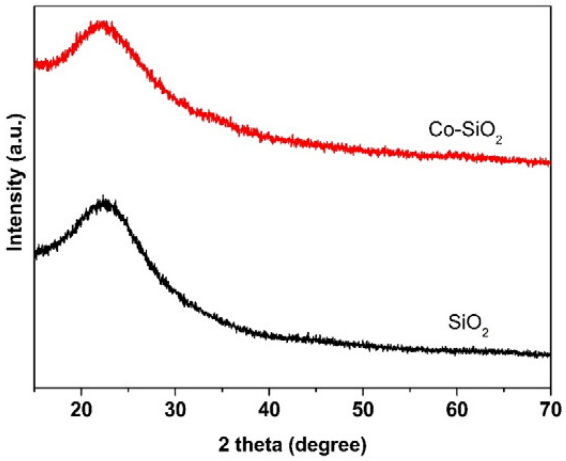


Fig. 3. XRD spectrum of pure $SiO_2$ aerogel and Co-$SiO_2$ aerogel.

alcogels was exposed to supercritical conditions for 1 hour 15 minutes (240 °C, 64 bars). The brownish appearance of the supercritical dried sample is shown in Fig. 2c. After calcination of the dried aerogel at 500 °C for 6 hours, the final nanocomposites were obtained (Fig. 2d), the appearance changes to a light violet color, which is then, characterized using different techniques. For comparison, a pure $SiO_2$ sample was obtained using the same procedure.

*Characterizations*

The effect of cobalt nanoparticles dispersion in silica hydrosol on various properties of pure $SiO_2$ aerogel samples such as packing density, microstructure, porosity, and textual properties was investigated using various methods such as micro-balance, field emission scanning electron microscopy (FE-SEM), powder X-ray diffraction (XRD), and $N_2$ adsorption-desorption (Brunauer-Emmett-Teller) [20-21]. Cu K radiation was used to detect the crystal structure of Co-$SiO_2$ aerogel using an XRD-6100 Lab device. With a scanning rate of 5° min, values of 2 were in the range of 10-80°. The surface modification of the Co-$SiO_2$ aerogel was verified using Fourier transform infrared (FTIR) spectroscopy with a Perkin Elmer (Model r 760). Solid samples were prepared using KBr as a diluent, and spectra with wavenumbers ranging from 400 to 4000 $cm^{-1}$ were obtained. A field emission scanning electron microscope (FE-SEM) was used to examine the microstructure and morphology of the Co-$SiO_2$ aerogel. The Brunauer-Emmett-Teller (BET) surface area analyzer determined the precise surface area ($S_{BET}$), pore size, and pore volume (Pv) of the Co-$SiO_2$ aerogel.

## RESULTS AND DISCUSSION

XRD spectra for Co-$SiO_2$ aerogel and pure $SiO_2$ aerogel samples are shown in Fig. 3. In pure $SiO_2$ aerogels and Co-$SiO_2$ nanocomposites samples, a single broad peak at diffraction angle 2q=24°

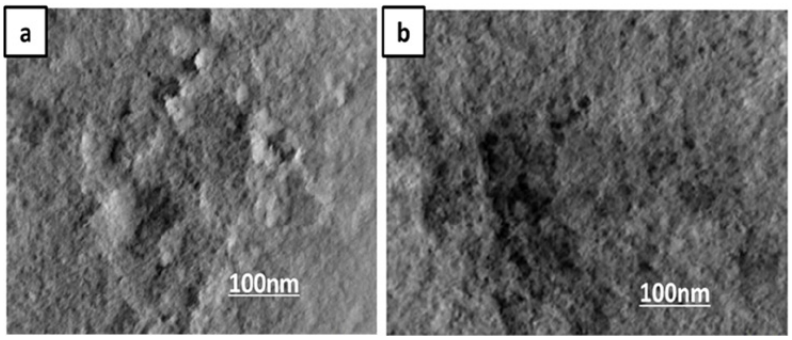


Fig. 4. SEM images of a) Pure $SiO_2$ aerogel and b) Co-$SiO_2$ aerogel.

Table 1. Comparison of textural properties of pure and Co-$SiO_2$ aerogels.

| Aerogel | Drying method | Total pore volume ($cm^3/g$) | Average pore diameter (A°) | BET surface area ($m^2/g$) | Ref. |
|---|---|---|---|---|---|
| Co-$SiO_2$ | Supercritical($N_2$) | 2.9 | 9 | 802 | This work |
| $SiO_2$ | Supercritical($N_2$) | 7.7 | 20 | 1134 | This work |
| V-silica | Supercritical($CO_2$) | 1.2 | 79 | 530 | [31] |
| Cu-silica | | 1.1 | 62 | 590 | |
| Nickel-silica aerogel | APD | | | 537–679 | [32] |
| Nickel-silica aerogel | Supercritical($N_2$) | 2.03 | 24 | 794 | [26] |
| SiCo(IFOH) | APD | 0.64 | 39 | 567 | [33] |
| SiCo(IFO) | | 0.54 | 43 | 425 | ,, |
| SiCo(LFO) | | 0.55 | 54 | 404 | ,, |

corresponds to the amorphous phase [22]. The samples pure $SiO_2$ and Co-$SiO_2$ exhibit no additional sharp peaks; this indicates that both the samples have amorphous pore structure. The absence of sharp peaks in Co-$SiO_2$ nanocomposites samples can be observed because of low concentration of cobalt nanoparticles in silica matrix [23].

FE-SEM was used to describe the morphologies and microstructures of the prepared Co-$SiO_2$ and $SiO_2$ aerogels samples, as shown in Fig. 4. The nanoporous structure of $SiO_2$ and Co-$SiO_2$ aerogel was visible in the FE-SEM images (Fig. 4a and 4b). The three-dimensional (3D) porous arrangement is made up of spongy silica clumps that represent the Co-$SiO_2$ microstructure [24-25]. In comparison to pure $SiO_2$ aerogel, Fig. 4 b indicates the large number of clumps of particles in Co-$SiO_2$ aerogel samples with higher density. As nanofillers, cobalt nanoparticles were incorporated into the silica matrix structure, which acts as a skeleton backbone to stabilize the silica aerogel**.**

Aerogels unique surface area ($S_{BET}$) and pore size are crucial in determining their adsorption properties. Therefore, in order to investigate the adsorption of Co-$SiO_2$ aerogel with the specific surface area and pore size, $N_2$ adsorption-desorption technique is applied. The impact of dispersion of cobalt nanoparticles particles in silica sol on textural properties like average pore size, surface area, cumulative open pore volume of the pure silica aerogel and Co-$SiO_2$ aerogel were derived from BET techniques are summarized in Table 1. In comparison to previously reported metal oxide based silica aerogels, the textural properties of prepared samples are superior shown in Table 1. Due to the regulated capillary pressure and supercritical drying at high pressure and temperature, the obtained sample had a spectacular surface area. The $N_2$ gas adsorption/ desorption isotherms and pore size distributions of pure $SiO_2$ aerogel and Co-$SiO_2$ aerogel were analyzed with BJH desorption isotherm method. The nitrogen adsorption-desorption isotherms obtained at 77 K are shown in Fig. 5. Fig. 5 shows that $SiO_2$ and Co-$SiO_2$ aerogels exhibit type-IV isotherms [26-27], demonstrating the mesoporous nature of pure $SiO_2$ and Co-$SiO_2$ aerogels. In addition, the hysteresis curve suggests type H2, which indicates the presence of spherical pores in both samples [28-29]. After supercritical drying, the large pore size of pure silica aerogel and Co-$SiO_2$ aerogel indicates the presence of a mesoporous

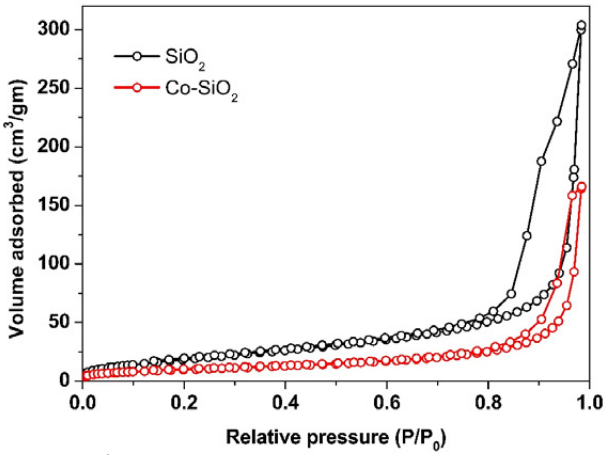


Fig. 5. $N_2$ absorption/desorption isotherms of pure $SiO_2$ aerogels and Co-$SiO_2$ aerogels.

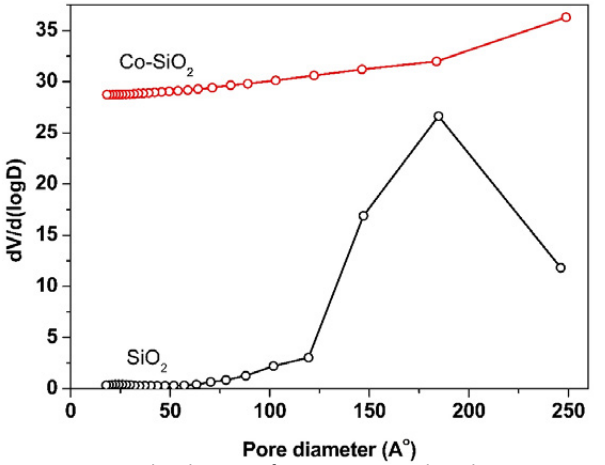


Fig. 6. BET pore size distributions of pure $SiO_2$ aerogels and Co-$SiO_2$ aerogels.

silica network. The obtained Co-$SiO_2$ aerogel has a lower $S_{BET}$, cumulative pore volume, and pore size distribution than the pure $SiO_2$ aerogel. The reduced porosity (percent), pore diameter, and surface area of Co-$SiO_2$ are due to the immersions of Co nanoparticles. The prominent peak in the $SiO_2$ aerogel is mostly in the mesoporous range (2-50 nm) [30]. With dispersion of Co nanoparticles as nanofiller into the $SiO_2$ matrix as support, the mesoporous morphology of $SiO_2$ has a negligible effect on the isotherms of Co-$SiO_2$. The average $S_{BET}$ and pore size may help to improve adsorption properties. The pore size distributions and $N_2$ gas adsorption/desorption isotherms of pure $SiO_2$ and Co-$SiO_2$ aerogels were investigated. In contrast to pure silica aerogel, the pore size distribution curves (Fig. 6) were slightly uniform, and pore diameter values shifted to smaller values, indicating that cobalt oxide nanoparticles resulted in uniform pore nature. PSD and pore volume of aerogel is affected by the ratio of silica sol to silica sol with cobalt (Table1).

FTIR analysis was used to investigate the functional groups and Si-O-Si bonds in Co-$SiO_2$ aerogel. In Fig. 7, the FTIR spectra of pure $SiO_2$ and Co-$SiO_2$ aerogels are shown. Fourier transforms infrared spectroscopy (FTIR) spectra of pure $SiO_2$ and Co-$SiO_2$ aerogels usually indicate the presence of chemical bonds with silylation surfaces. In Fig. 7 shows the peak at 1070 and 495 $cm^{-1}$ related to the Si—O—Si stretching vibrations representing the assembly of silica networks [34]. The wide absorption crest centered at 3450 $cm^{-1}$ and 1630 $cm^{-1}$ due to the Si-OH absorption range associated due to the existence of water [35]. The non-calcined Co-$SiO_2$ aerogels FTIR spectra show no peaks of cobalt oxide particles, but a peak at 810 $cm^{-1}$suggests the existence of nitrate groups.

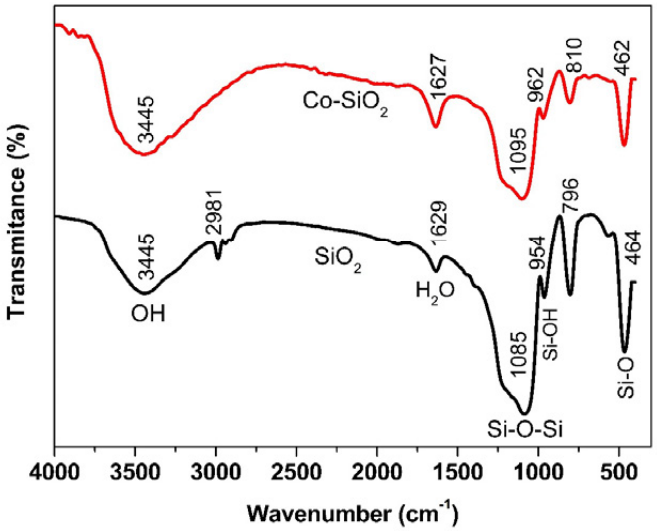


Fig. 7. FTIR spectra of pure $SiO_2$ aerogels and Co-$SiO_2$ aerogels.

## CONCLUSIONS

We successfully prepared the mesoporous Co-$SiO_2$ aerogel from colloidal dispersions of cobalt nanoparticles with sol-gel emulsion of tetraethoxysilane (TEOS) via $N_2$ supercritical drying technique. The immersion of the cobalt based silica sol was possible under precise investigational circumstances including ratio of solvent, pH value and temperature to avoid both the suspension and the agglomeration due to presence of the cobalt nanoparticles while reacting. Homogeneous colloidal dispersion also obtained significant features for implementation as a catalyst such as large surface area, highly porous, homogeneous nanostructure within the silica network. A value of BET specific surface area 802 $m^2/g$, was obtained for Co-$SiO_2$ aerogel, the large pore size was achieved up to 9 nm for the Co-$SiO_2$ aerogel. The spectrum of FTIR study indicates the existence of the Si–$CH_3$ group which indicates hydrophobic nature of Co-$SiO_2$ aerogel. Using silica aerogel network as a host for CoNPs slightly decreases the surface area, surface volume, and commutative pore volume and pore size of the pure silica aerogel matrix. Presence of CoNPs percentage within the silica matrix affects the transparency of $SiO_2$ aerogels. Further studies are presently ongoing to resolve the effect of CoNPs on the silica matrix. In addition, we will further investigate the physico-chemical properties of CoNPs-$SiO_2$ aerogels nanomaterials for commercialization.

## ACKNOWLEDGEMENT

Pradip Sarawade acknowledges University of Mumbai under minor research project, Department of Physics, University of Mumbai and SERB grants (EEQ/2020/0002980) under DST for their financial support.

## CONFLICT OF INTERESTS

There is no conflict of interest.

## REFERENCES

1. Shinde R. A., Aadole V. A., (2021), Anti-microbial evaluation, experimental and theoretical insights into molecular structure, electronic properties, and chemical reactivity of (E)-2-((1H-indol-3-yl) methylene)-2, 3-dihydro-1H-inden-1-one. *Appl. Organomet. Chem.* 2: 48-58.
2. Sahebnasagh S., Fadaee Kakhki J., Ebrahimi M., Bozorgmehr M., Abedi M., (2021), Pre-concentration and determination of fluoxetine in hospital wastewater and human hair samples using solid-phase μ-extraction by Silver nanoparticles followed by spectro-fluorimetric. *Chem. Methodol.* 5: 211-218.
3. Farhadi B., Ebrahimi M., Morsali A., (2021), Microextraction and determination Trace amount of propranolol in aqueous and pharmaceutical samples with oxidized multi-walled carbon nanotubes. *Chem. Methodol.* 5: 227-233.
4. Fazal-ur-Rehman M., Qayyum I., (2020), Biomedical scope of gold nanoparticles in medical sciences; an advancement in cancer therapy. *J. Medic. Chem. Sci.* 3:399-407.
5. Nabipour H., Hu Y., (2020), Nanohybrid based on layered zinc hydroxide with salicylic acid drug: Investigation of the structure and controlled release properties. *J. Medic. Chem. Sci.* 3: 235-244.
6. Deng X., Tuysuz H., (2014), Cobalt-oxide-based materials as water oxidation catalyst: Recent progress and challeng-

es. *ACS Catal.* 4: 3701-3714.
7. Dhawale D., Bodhankar P., Sonawane N., Sarawade P. B., (2019), Fast microwave-induced synthesis of solid cobalt hydroxide nanorods and their thermal conversion into porous cobalt oxide nanorods for efficient oxygen evolution reaction. *Sustain. Energy & Fuels.* 3: 1713-1719.
8. Bodhankar P., Chunduri A., Dhawale D. S., Sarawade P. B., Vinu A., (2019), Fine-tuning the water oxidation performance of hierarchical $Co_3O_4$ nanostructures prepared from different cobalt precursors. *Sustain. Energy & Fuels.* 5: 1120-1128.
9. Warang T., Fernandes R., Bazzanella N., Miotello A., (2013), $Co_3O_4$ nanoparticles assembled coatings synthesized by different techniques for photo-degradation of methylene blue dye. *Appl. Catal. B*. 132-133: 204-211.
10. Lou Y., Wang L., Zhao Z., Zhang Y., Zhang Z., Lu G., Guo Y., (2014), Low-temperature CO oxidation over $Co_3O_4$-based catalysts: Significant promoting effect of $Bi_2O_3$ on $Co_3O_4$ catalyst. *Appl. Catal. B*. 146: 43-49.
11. Amonette J. E., Matyáš J., (2017), Functionalized silica aerogels for gas-phase purification, sensing, and catalysis: A review. *Microp. Mesop. Mater.* 250: 100-119.
12. Tai Y., Tajiri K., (2008), Preparation, thermal stability, and CO oxidation activity of highly loaded Au/titania-coated silica aerogel catalysts. *Appl. Catal. A: General.* 342: 113-118.
13. Yousefi Amiri T., Moghaddas J., (2015), Cogeled copper–silica aerogel as a catalyst in hydrogen production from methanol steam reforming. *Int. J. Hydrogen Energy.* 40: 1472-1480.
14. Lin Q., Yang G., Chen Q., Fan R., Yoneyama Y., Wan H., Tsubaki N., (2015), Design of a hierarchical meso/macroporous zeolite-supported cobalt catalyst for the enhanced direct synthesis of isoparaffins from syngas. *Chem. Cat. Chem.* 7: 682-689.
15. Bittner M., Helmich L., Nietschke F., Geppert B., Oeckler O., Feldhoff A., (2017), Porous $Ca_3Co_4O_9$ with enhanced thermoelectric properties derived from Sol–Gel synthesis. *J. Eur. Ceram. Soc.* 37: 3909-3915.
16. Kahraman F., Madre M. A., Rasekh S., Salvador C., Bosque P., Torres M. A., Diez J. C., Sotelo A., (2015), Enhancement of mechanical and thermoelectric properties of $Ca_3Co_4O_9$ by Ag addition. *J. Europ. Ceram. Soc.* 35: 3835-3841.
17. Khedkar M. V., Somvanshi S. B., Humbe A. V., Jadhav K. M., (2019), Surface modified sodium silicate based superhydrophobic silica aerogels prepared via ambient pressure drying process. *J. Non-Crystalline Solids.* 511: 140-146.
18. Ji X., Zhou Q., Qiu G., Yue C., Guo M., Chen F., Zhang M., (2018), Preparation of monolithic silica-based aerogels with high thermal stability by ambient pressure drying. *Ceram. Int.* 44: 11923-11931.
19. Jadhav S., Sarawade P., (2020), Synthesis and characterization of Nickel nitrate as additive into $SiO_2$ matrix by supercritical drying method. *Available at SSRN 3567113*.
20. Sarawade P. B., Kim J-K., Hilonga A., (2010), Production of low-density sodium silicate-based hydrophobic silica aerogel beads by a novel fast gelation process and ambient pressure drying process. *Solid State Sci*. 12: 911-918.
21. Sarawade P. B., Kim J-K., Kim H-K., (2007), High specific surface area TEOS-based aerogels with large pore volume prepared at an ambient pressure. *Appl. Surf. Sci.* 254: 574-579.
22. Sarawade P. B., Shao G. N., Quang D. V., Kim H. T., (2013), Effect of various structure directing agents on the physicochemical properties of the silica aerogels prepared at an ambient pressure. Appl. Surf. Sci. 287: 84-90.
23. Li J., Xu X., Hao Zh., (2008), Mesoposous silica supported cobalt oxide catalytic removal of benzene. *J. Porous Mater.* 15: 163-169.
24. Bhagat S. D., Kim Y-H., Ahn Y-S., (2006), Textural properties of ambient pressure dried water-glass based silica aerogel beads: One day synthesis. *Microp. Mesop. Mater.* 96: 237-244.
25. Sarawade P. B., Quang D. V., Hilonga A., (2012), Synthesis and characterization of micrometer-sized silica aerogel nanoporous beads. *Mater. Lett.* 81: 37-40.
26. Sarawade P. B., Kim J. K., Park J. K., (2006), Influence of solvent exchange on the physical properties of sodium silicate based aerogel prepared at ambient pressure. *Aeros. and Air Quality Res.* 6: 93-105.
27. Sarawade P. B., (2011), Nanostructured silica aerogel. *LAP Lambert Academic Pub.* AG & Company KG.
28. Hilonga A., Kim J. K., Sarawade P. B., (2009), Reinforced silver-embedded silica matrix from the cheap silica source for the controlled release of silver ions. *Appl. Surf. Sci.* 255: 8239-8245.
29. Hilonga A., Kim J. K., Sarawade P. B., (2010), Mesoporous titania–silica composite from sodium silicate and titanium oxychloride. Part II: One-pot co-condensation method. J. Mater. Sci. 45: 1264-1271.
30. Al-Oweini R., El-Rassy H., (2009), Synthesis and characterization by FTIR spectroscopy of silica aerogels prepared using several $Si(OR)_4$ and $R''Si(OR')_3$ precursors. *J. Molec. Struc.* 919: 140-145.
31. Hair L. M., Owens L., Tillotson T., (1995), Local, nano- and micro-structures of mixed metal oxide aerogels for catalyst applications. *J. Non-Cryst. Solids.* 186: 168-176.
32. Han X., Williamson F., Bhaduri G. A., (2015), Synthesis and characterisation of ambient pressure dried composites of silica aerogel matrix and embedded nickel nanoparticles. *J. Supercrit. Fluids.* 106: 140-144.
33. Santos G. A., Santos C. M. B., Da Silva S. W., (2012), Sol–gel synthesis of silica–cobalt composites by employing $Co_3O_4$ colloidal dispersions. *Collo. Surf. A: Physicochem. Eng. Aspec.* 395: 217-224.
34. Liang Y., Ouyang J., Wang H., (2012), Synthesis and characterization of core–shell structured $SiO_2$@$YVO_4$ : $Yb^{3+}$, $Er^{3+}$ microspheres. *Appl. Surf. Sci.* 258: 3689-3694.
35. Sarawade P. B., Kim J. K., Hilonga A., (2010), Recovery of high surface area mesoporous silica from waste hexafluorosilicicacid ($H_2SiF_6$) of fertilizer industry. *J. Hazard. Mater.* 173: 576-580.